RESEARCH ARTICLE

Quantifying infectious disease epidemic risks: A practical approach for seasonal pathogens

Alexander R Kaye[1,2]*, **Giorgio Guzzetta**[3], **Michael J Tildesley**[1,2,4], **Robin N Thompson**[5]

1 Mathematics Institute, University of Warwick, Coventry, United Kingdom, **2** Zeeman Institute for Systems Biology and Infectious Disease Epidemiology Research (SBIDER), University of Warwick, Coventry, United Kingdom, **3** Centre for Health Emergencies, Bruno Kessler Foundation, Trento, Italy, **4** School of Life Sciences, University of Warwick, Coventry, United Kingdom, **5** Mathematical Institute, University of Oxford, Oxford, United Kingdom

* a.kaye@warwick.ac.uk
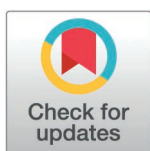
Abstract

For many infectious diseases, the risk of outbreaks varies seasonally. If a pathogen is usually absent from a host population, a key public health policy question is whether the pathogen's arrival will initiate local transmission, which depends on the season in which arrival occurs. This question can be addressed by estimating the "probability of a major outbreak" (the probability that introduced cases will initiate sustained local transmission). A standard approach for inferring this probability exists for seasonal pathogens (involving calculating the Case Epidemic Risk; CER) based on the mathematical theory of branching processes. Under that theory, the probability of pathogen extinction is estimated, neglecting depletion of susceptible individuals. The CER is then one minus the extinction probability. However, as we show, if transmission cannot occur for long periods of the year (e.g., over winter or over summer), the pathogen will most likely go extinct, leading to a CER that is equal (or very close) to zero even if seasonal outbreaks can occur. This renders the CER uninformative in those scenarios. We therefore devise an alternative approach for inferring outbreak risks for seasonal pathogens (involving calculating the Threshold Epidemic Risk; TER). Estimation of the TER involves calculating the probability that introduced cases will initiate a local outbreak in which a threshold number of cumulative infections is exceeded before outbreak extinction. For simple seasonal epidemic models, such as the stochastic Susceptible-Infectious-Removed model, the TER can be calculated numerically (without model simulations). For more complex models, such as stochastic host-vector models, the TER can be estimated using model simulations. We demonstrate the application of our approach by considering chikungunya virus in northern Italy as a case study. In that context, transmission is most likely in summer, when environmental conditions promote vector abundance. We show that the TER provides more useful assessments of outbreak risks than the CER, enabling practically relevant risk quantification for seasonal pathogens.

Author summary

Invasive pathogens pose a substantial challenge to human health, particularly as outbreak risks for some infectious diseases are being exacerbated by climate change. For example, the occurrence of seasonal vector-borne disease outbreaks in mainland Europe is increasing, even though pathogens like the chikungunya and dengue viruses are not normally present there. In this changing landscape, assessing the risk posed by invasive pathogens requires computational methods for estimating the probability that introduced cases will lead to a local outbreak, as opposed to the first few cases fading out without causing a local outbreak. In this article, we therefore provide a computational framework for estimating the risk that introduced cases will lead to a local outbreak in which a pre-specified, context specific threshold number of cases is exceeded (we term this risk the "Threshold Epidemic Risk", or TER). Since even small seasonal outbreaks can have negative impacts on local populations, we demonstrate that calculation of the TER provides more practically relevant estimates of local outbreak risks than those inferred using standard methods. Going forwards, our computational modelling framework can be used to assess outbreak risks for a wide range of seasonal diseases.

1. Introduction

Even if a pathogen is not commonly present in a host population, there remains a risk that imported cases will lead to local transmission [1–5]. In southern Europe, for example, vector-borne diseases such as dengue and chikungunya are not endemic, yet outbreaks occur due to pathogen importation followed by autochthonous (i.e., local) transmission [6–8]. The risk that imported cases will lead to a substantial local outbreak, as opposed to sporadic onwards transmissions occurring, varies seasonally. This is because factors such as host behaviour, pathogen survivability and vector ecological dynamics change during the year, and are affected by weather variables such as temperature, rainfall and humidity [9–12]. It is useful to identify times of year at which outbreaks are most likely, and to provide quantitative estimates of temporally varying outbreak risks, to inform vector or pathogen surveillance and control interventions.

Previous work on the topic of inferring the risk that introduced cases will initiate sustained local transmission has focussed on estimating the so-called "probability of a major outbreak", based on the number of imported cases and the transmissibility of the pathogen. This probability can be inferred both for pathogens that are transmitted directly between hosts [13–26] and those that are spread via vectors [27–30]. Furthermore, the probability of a major outbreak has been calculated in systems in which transmission parameter values are assumed to be constant [8,30–33] and those in which temporal variations in transmission are accounted for [29,34–41]. Estimates of the probability of a major outbreak have been generated using approximations of a wide range of epidemiological models, including SIS, SIR and SEIR models [30,31], spatial models [22,23,27], models with host demography [25,26,42] and models that relax the standard assumption that epidemiological time periods are drawn from exponential distributions [24,43]. In addition, calculations of the probability of a major outbreak have been undertaken for a wide variety of diseases, including COVID-19 [21,32], Ebola [31,43] and dengue [8,44].

In all these different settings, the probability of a major outbreak is typically derived by assuming that infections are generated according to a branching process [45], neglecting depletion of susceptible individuals (i.e., assuming that there is a constant supply of

susceptible hosts available for each infected individual to infect). When transmission parameter values do not vary temporally, under this assumption a pathogen either goes extinct following its introduction or the number of infections grows unboundedly. The probability of a major outbreak calculated in this way corresponds to the probability that the second of these scenarios arises (i.e., that infinitely many infections occur in the branching process model). Generally, this is appropriate, and estimates of the probability of a major outbreak match the proportion of simulations of stochastic compartmental models (that account for depletion of susceptible individuals) in which "large" outbreaks occur, at least when parameters take constant values and R_0 is sufficiently larger than one [29,30]. However, the use of branching process theory to estimate outbreak risks can be problematic when transmission is seasonal.

Specifically, when transmission can only occur during some periods of the year, the pathogen is highly likely to go extinct in seasons when environmental conditions are unsuitable for transmission. Consequently, even with a constant supply of susceptible individuals for infected hosts to infect, the number of infections will not grow indefinitely. As a result, standard analytic estimates of the probability of a major outbreak (here called the Case Epidemic Risk, or CER, following the use of this terminology previously for pathogens for which transmission varies temporally [29]) are either zero or vanishingly small (we use the term "vanishingly small" to refer to values that are positive but very close to zero [40]). Since pathogen extinction is highly likely to occur, a more practically relevant question is how many infections will there be before extinction? If a substantial number of infections arises prior to pathogen extinction, we contend that an outbreak should still be classified as "major".

Here, we therefore provide a metric for calculating the probability of a major outbreak for seasonal pathogens. Specifically, we calculate the probability that, following the introduction of a pathogen to a host population, a pre-specified, context dependent threshold number of cumulative infections is exceeded. We refer to this metric as the Threshold Epidemic Risk (TER). This metric can be calculated using stochastic compartmental transmission models that account for both seasonality and depletion of susceptible individuals, and throughout this article we compare calculations of the TER to analogous values of the CER. A schematic is shown in Fig 1, illustrating that when transmission varies seasonally (Fig 1A) then outbreaks may be likely to fade out as soon as a season arrives that is not conducive to transmission (leading to a CER that is either zero or vanishingly small; Fig 1B). However, even in that scenario, seasonal outbreaks may still lead to substantial numbers of cases (the TER may be larger than zero; Fig 1C).

First, we show how the TER can be calculated numerically (i.e., through the numerical solution of a system of equations, without requiring model simulations) for the stochastic SIR model with seasonally varying transmission. Then, we show how the TER can be calculated for more complex models using stochastic simulations by considering a stochastic host-vector model of chikungunya virus transmission in northern Italy. When transmission is possible all year round, the TER and CER can give similar estimates. However, for both models, when there are substantial periods of the year during which sustained transmission is not possible, the difference between outbreak risk estimates arising from these two metrics can be large. For chikungunya virus, which is spread by *Aedes albopictus* [46], there are long periods of the year in northern Italy during which vector abundance is too low for virus transmission [8]. Consequently, the CER is low (either zero or vanishingly small), yet major outbreaks due to local transmission can sometimes occur, depending on the precise definition of a "major outbreak" used. Since a policy-maker can choose a practically relevant threshold when estimating the TER, it is a useful metric to consider when quantifying seasonal outbreak risks as an aid for public health policy making.
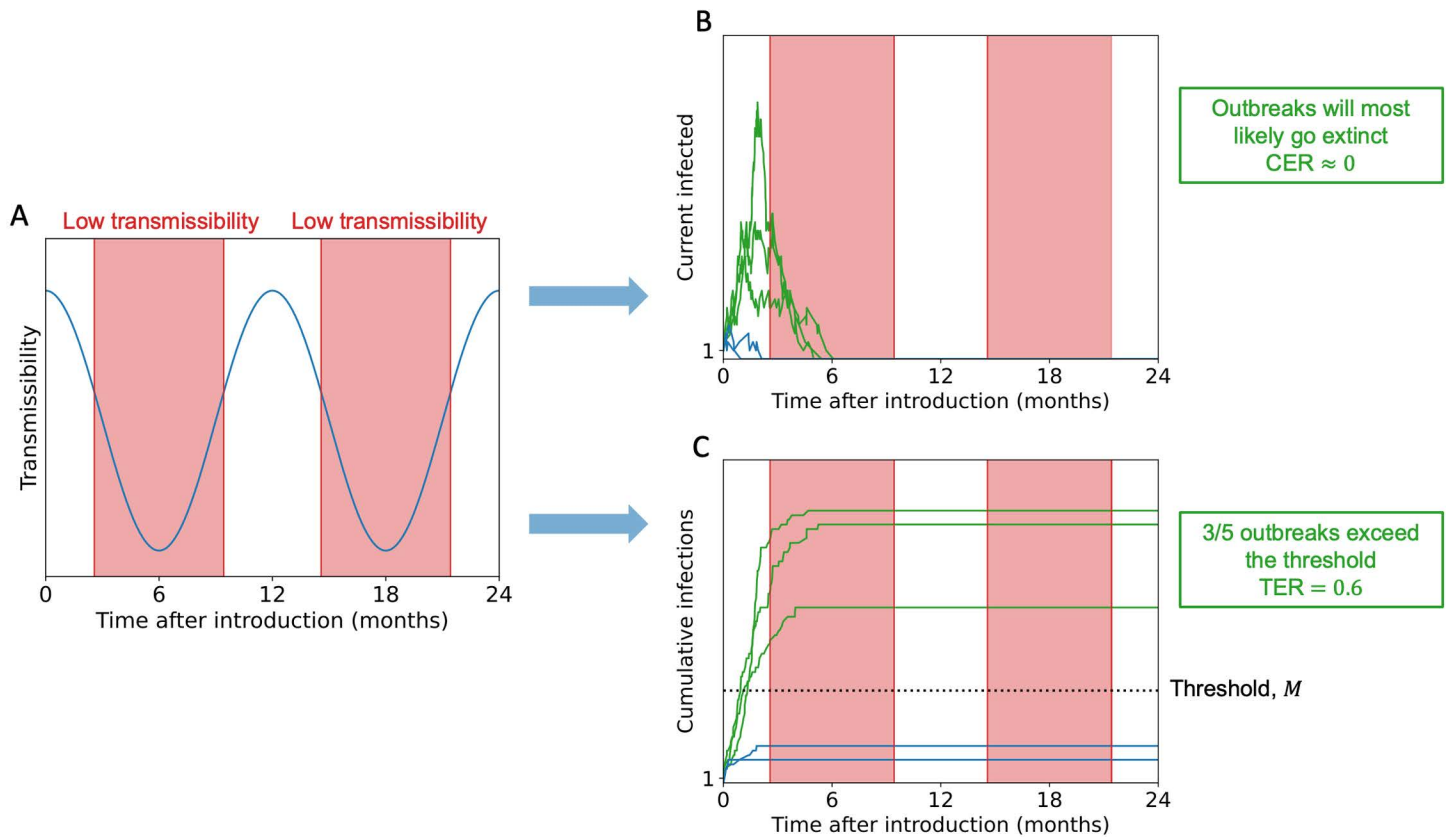
Fig 1. Schematic illustrating the difference in outbreak risk assessments for seasonal pathogens obtained using the CER and TER. A. Seasonal pathogen transmission comprises of periods of high and low transmissibility (low transmissibility periods, during which sustained pathogen transmission is impossible, are shaded in red). B. In the scenario considered here, outbreaks are highly likely to go extinct during low transmissibility periods. As a result, the CER suggests that major outbreaks will not occur. C. Despite the value of the CER, there is the potential for some outbreaks to generate a substantial number of cases. In this illustrative example, three out of every five outbreaks generate numbers of cases that exceed a pre-specified threshold, M, leading to a TER value of 0.6. In panels B and C, outbreaks in which at least M cumulative infections occur are plotted in green and those with fewer than M cumulative infections are plotted in blue.

https://doi.org/10.1371/journal.pcbi.1012364.g001

2. Methods

2.1. Epidemiological models

2.1.1. SIR model. The ordinary differential equation (ODE) version of the Susceptible-Infectious-Removed (SIR) model with time-dependent infection and removal rates is:

$$\frac{dS(t)}{dt} = -\frac{\beta(t)S(t)I(t)}{N},$$

$$\frac{dI(t)}{dt} = \frac{\beta(t)S(t)I(t)}{N} - \gamma(t)I(t),$$

$$\frac{dR(t)}{dt} = \gamma(t)I(t). \tag{1}$$

In this model, $S(t)$ is the number of individuals who are susceptible to the pathogen at time t, $I(t)$ is the number of infectious individuals, and $R(t)$ is the number of removed individuals (including those who have recovered and become immune and those who have died). The total population size, $S(t) + I(t) + R(t) = N$, is constant under this model. The transmission rate is denoted by $\beta(t)$ and the removal rate is denoted by $\gamma(t)$. In our analyses, the analogous stochastic model is considered, and simulations are run using a modified version of the Gillespie direct method [47] in which time-dependent rates are accounted for [29,48,49] (Algorithm A in S1 Text). For this model, the instantaneous basic reproduction number is given by $R_0(t) = \dfrac{\beta(t)}{\gamma(t)}$.

Time t is measured in months and the infection rate is chosen to be periodic with a period of 12 months:

$$\beta(t) = \max\left(\beta_0 + \beta_1 \cos\left(\frac{\pi}{6}t - \phi\right), 0\right). \tag{2}$$

The removal rate is assumed to be constant ($\gamma(t) = \gamma$). We use these specific forms of the infection and removal rates in our analyses but our approach for computing the TER can be applied for any functions $\beta(t)$ and $\gamma(t)$ (the functions do not even need to be periodic). The parameter values used are shown in the captions to Figs 2–4.

2.1.2. Chikungunya transmission model. We adapt the ODE model of chikungunya virus transmission described by Guzzetta *et al.* [8,44]. Specifically, we separate the vector ecological dynamics from the host-vector epidemiological dynamics. The ecological model is given by:

$$\frac{dE}{dt} = n_E d_V\left(T(t)\right)N_V - \left(m_E\left(T(t)\right) + d_E\left(T(t)\right)\right)E,$$

$$\frac{dL}{dt} = d_E\left(T(t)\right)E - \left[m_L\left(T(t)\right)\left(1 + \frac{L}{a_s}\right) + d_L\left(T(t)\right)\right]L,$$

$$\frac{dP}{dt} = d_L\left(T(t)\right)L - \left(m_P\left(T(t)\right) + d_P\left(T(t)\right)\right)P,$$

$$\frac{dN_V}{dt} = \frac{1}{2}d_P\left(T(t)\right)P - m_V\left(T(t)\right)N_V. \tag{3}$$

In this model, the population of vectors (*Ae. albopictus*) is split into eggs (E), larvae (L), pupae (P) and adults (N_V). For notational convenience, we do not denote the dependence of these state variables on t in the equations above explicitly, although the number of vectors in each compartment of the model varies temporally. The parameter d_X (for $X = E, L$ or) represents the development rate in compartment X (e.g., d_E is the rate at which eggs develop into larvae) and the parameter m_X (for $X = E, L$ or) represents the baseline mortality rate in compartment X. The parameter m_V represents the rate at which adult vectors die. The parameter d_V represents the rate of egg deposition for female adults with an average number of eggs, n_E, per adult female oviposition. The effect of overcrowded breeding sites on the larval mortality rate is dictated by the overcrowding parameter, a_s, which was fitted to on site capture data by Guzzetta *et al.* [8,44]. The factor of $1/2$ in the equation for N_V reflects the

fact that we only track adult female vectors, since male vectors do not spread the virus. The spatial scale of the model is assumed to be a single hectare (so that N_V represents the number of adult female vectors in one hectare).

The temperature, $T(t)$, is assumed to vary seasonally (i.e., with period 12 months):

$$T(t) = T_0 + T_1 \cos\left(\frac{\pi}{6}t - \psi\right).$$ (4)

The values of T_0 (mean temperature), T_1 (amplitude of the temperature oscillations) and ψ (phase shift) are determined by fitting $T(t)$ to daily mean temperature data (measured in Celsius) from Feltre, a town in northern Italy, separately for 2014 and 2015, using least squares estimation. The temperature data were obtained from MODIS satellite Land Surface Temperature measurements as detailed in [8]. In our analysis of the temperature data from 2014, time $t = 0$ corresponds to 1st April 2014. In our analysis of the data from 2015, time $t = 0$ corresponds to 1st April 2015.

We solve the ecological model (system of equations (3)) numerically to obtain $N_V(t)$. To facilitate straightforward computation of the CER (see below), we then fit a skewed and scaled Gaussian to the monthly values of $N_V(t)$ using least squares estimation, and use the resulting fitted version of $N_V(t)$ in all of our analyses. Again, we perform this fitting separately for 2014 and 2015. The fitted curve is of the form:

$$N_V(t) = AB^{-\frac{(t-C)^2}{D}}\left[1 + \mathrm{erf}\left(\frac{t-C}{E}\right)\right],$$ (5)

in which erf is the error function. Equation (5) is a skewed, scaled, and shifted Gaussian, chosen because of its resemblance to the output of the deterministic ecological model (S1C and S1D Fig). By considering the deterministic version of the ecological model, we avoid running stochastic simulations of the ecological model, which would be computationally expensive due to the large number of events that would arise in that system.

Stochastic epidemiological dynamics are then simulated using a stochastic host-vector model. The analogous deterministic model to the stochastic model that we consider is:

$$\frac{dS_V}{dt} = -k\beta_V\frac{S_V I_H}{N} - m_V(T(t))S_V,$$

$$\frac{dE_V}{dt} = k\beta_V\frac{S_V I_H}{N} - \left(\frac{1}{\omega_V} + m_V(T(t))\right)E_V,$$

$$\frac{dI_V}{dt} = \frac{1}{\omega_V}E_V - m_V(T(t))I_V,$$

$$\frac{dS_H}{dt} = -k\beta_H\frac{S_H I_V}{N},$$

$$\frac{dI_H}{dt} = k\beta_H\frac{S_H I_V}{N} - \frac{1}{\tau}I_H,$$

$$\frac{dR_H}{dt} = \frac{1}{\tau}I_H.$$ (6)

The compartments represent the numbers of susceptible, exposed and infectious vectors (S_V, E_V and I_V, respectively) along with the numbers of susceptible, infectious and removed hosts (S_H, I_H and R_H, respectively). In this model, it is assumed that, after entering the I_V compartment, an adult female vector remains infectious for life. The parameter k represents the vector bite rate. The per-bite probability of pathogen transmission from an infectious host to a susceptible vector is then denoted by β_V, with corresponding parameter β_H for transmission from an infectious vector to a susceptible host. The (mean) extrinsic incubation period is denoted by ω_V, the period for which an infectious host remains infected is τ, and N represents the host population size. The temperature-dependent parameters in both systems of equations (3) and (6) are explicitly labelled as functions of temperature, T, which itself varies temporally. In addition to the explanations here, each of the parameters in systems of equations (3) and (6) are listed in Table A in S1 Text, alongside their definitions and the values used in our analyses (including the functional forms of the temperature-dependent parameters).

Unlike the total host population size, which remains constant ($S_H + I_H + R_H = N$), the vector population size, N_V, varies with temperature and therefore varies temporally (equation (5)). The instantaneous basic reproduction number, $R_0(t)$, for this system is [8]:

$$R_0(t) = k^2 \beta_H \beta_V \frac{\tau}{m_V(T(t))} \frac{N_V}{N} \frac{1}{1 + \omega_V m_V(T(t))}. \tag{7}$$

When we run simulations of the analogous stochastic model to system of equations (6), we again adapt the Gillespie direct method [47] (Algorithm B in S1 Text). We assume that transmission parameters take constant values within each day (given by their values at the start of the day). We are therefore able to use the Gillespie direct method within each day. At the end of each day, we compare the total vector population size, $S_V + E_V + I_V$, with N_V (as determined by equation (5)). If $S_V + E_V + I_V < N_V$, then we assume that new susceptible vectors are born (i.e., we increase S_V) until $S_V + E_V + I_V = N_V$. If instead $S_V + E_V + I_V > N_V$, we select vectors uniformly at random to die until $S_V + E_V + I_V = N_V$, since the per-vector death rates in system of equations (6) are equal for each of the S_V, E_V and I_V compartments. By following this procedure, we simulate stochastic epidemiological dynamics while remaining consistent with the deterministic ecological dynamics (system of equations (3) and equation (5)).

2.2. Case Epidemic Risk (CER)

As described in the Introduction, a standard approach for estimating the probability of a major outbreak exists, involving the assumptions that infections occur according to a branching process and a constant supply of susceptible individuals is available for each infectious host to infect. This approach has been used previously in the context of pathogens for which transmission parameters vary temporally (e.g., [29,34,40]). Here, we refer to the probability of a major outbreak calculated in this way as the CER, following the use of this terminology in our earlier work [29]. In this section, we describe how the CER can be calculated for the stochastic SIR model and the stochastic host-vector model of chikungunya virus transmission.

2.2.1. SIR model. For the stochastic SIR model, if a single infectious individual enters the host population at time t_0, then the CER is given by [29,34,40]:

$$CER(t_0) = \frac{1}{1 + \int_{t_0}^{\infty} \gamma(r) e^{\int_{t_0}^{r} \beta(s) - \gamma(s) \mathrm{d}s} \, \mathrm{d}r}. \tag{8}$$

A derivation of this expression can be found in Section 2.3.1 of [29].

2.2.2. Chikungunya transmission model. To compute the CER for the host-vector model of chikungunya virus transmission, we use the method described in [29]. We denote the probability of a major outbreak occurring, if there are i infectious hosts, j exposed vectors and k infectious vectors at time t, by $p_{ijk}(t)$.

Assuming that the virus is introduced into the population at time t_0 by a single infectious host, then the CER is given by $p_{100}(t_0)$. Calculation of the CER then involves solving the following system of ODEs:

$$\frac{\mathrm{d}p_{100}(t)}{\mathrm{d}t} = \frac{k\beta_V N_V(t)}{N}\big[p_{100}(t)-1\big]p_{010}(t) + \frac{1}{\tau}p_{100}(t),$$

$$\frac{\mathrm{d}p_{010}(t)}{\mathrm{d}t} = -\frac{1}{\omega_V}p_{001}(t) + \left[m_V(t) + \frac{1}{\omega_V}\right]p_{010}(t),$$

$$\frac{\mathrm{d}p_{001}(t)}{\mathrm{d}t} = k\beta_H p_{100}(t)\big[p_{001}(t)-1\big] + m_V(t)p_{001}(t). \tag{9}$$

The first of these equations is derived in Section C of S1 Text, with the derivation of the remaining two following an identical procedure. We solve system of equations (9) numerically using the Chebfun open source MATLAB software package [50], with periodic boundary conditions ($p_{100}(0) = p_{100}(12)$, $p_{010}(0) = p_{010}(12)$ and $p_{001}(0) = p_{001}(12)$, where t is measured in months here). Chebfun requires the coefficients on the right-hand-side of system of equations (9) to be provided in functional forms (as functions of t, rather than vectors of values), necessitating our decision to use a functional form for $N_V(t)$ (equation (5)).

2.3. Threshold Epidemic Risk (TER)

Here, we describe how the TER can be calculated for the stochastic SIR model and stochastic host-vector model of chikungunya virus transmission. The TER represents the probability that, if a single infected individual (for the host-vector model, a single infected host) enters the population at time t_0, an outbreak occurs in which a threshold number (denoted M) of cumulative infections is exceeded (or equalled). For the host-vector model, this threshold refers to host infections, rather than vector infections.

2.3.1. SIR model. For the stochastic SIR model, we calculate the TER numerically, without resorting to model simulation. To do this, we choose a time, t_{max}, that is longer than any outbreak could potentially be. We then denote the probability that the number of cumulative infections exceeds or equals M prior to time t_{max}, given that there are I^* infectious individuals and R^* removed individuals in the population at time t, by $q_M(I^*, R^*, t)$.
In other words:

$$q_M(I^*, R^*, t) = P\big(I(t_{max}) + R(t_{max}) \geq M \,\big|\, I(t) = I^*, R(t) = R^*\big). \tag{10}$$

By choosing t_{max} to be longer than the timescale of any local outbreak, $q_M(I^*, R^*, t)$ is equivalent to the probability that at least M cumulative infections occur prior to outbreak extinction.

We discretise the time interval $[0, t_{max}]$ into n time steps, each of length Δt, where Δt is chosen to be small (by choosing n to be large) so that at most one event occurs in any time

interval of length Δt. By conditioning on the possible events occurring in the interval $(i\Delta t$, $(i+1)\Delta t]$, for $i = 0,1,\ldots,\frac{t_{\max}}{\Delta t} - 1$, we obtain:

$$
\begin{aligned}
q_M(I^*,R^*,i\Delta t) &= \mathbf{P}(\text{infection event in interval } (i\Delta t,(i+1)\Delta t])q_M\left(I^*+1,R^*,(i+1)\Delta t\right) \\
&\quad + \mathbf{P}(\text{removal event in interval } (i\Delta t,(i+1)\Delta t])q_M\left(I^*-1,R^*+1,(i+1)\Delta t\right) \\
&\quad + \mathbf{P}(\text{no event in interval } (i\Delta t,(i+1)\Delta t])q_M\left(I^*,R^*,(i+1)\Delta t\right) \\
&= \beta(i\Delta t)\frac{\left(N-I^*-R^*\right)I^*}{N}\Delta t q_M\left(I^*+1,R^*,(i+1)\Delta t\right) \\
&\quad + \gamma(i\Delta t)I^*\Delta t q_M\left(I^*-1,R^*+1,(i+1)\Delta t\right) \\
&\quad + \left(1-\beta(i\Delta t)\frac{\left(N-I^*-R^*\right)I^*}{N}\Delta t - \gamma(i\Delta t)I^*\Delta t\right)q_M\left(I^*,R^*,(i+1)\Delta t\right).
\end{aligned}
\tag{11}
$$

Since the outbreak will definitely have ended by time $t_{\max}$, we note that:

$$
q_M\left(I^*,R^*,t_{\max}\right) = \begin{cases} 1, I^*+R^* \geq M \\ 0, I^*+R^* < M \end{cases}.
\tag{12}
$$

enabling us to solve system of equations (11) backwards in time to find the values of $q_M\left(I^*,R^*,i\Delta t\right)$ for all values of I^*, R^* and i. In other words, we first compute $q_M\left(I^*,R^*,\left(\frac{t_{\max}}{\Delta t}-1\right)\Delta t\right)$, then $q_M\left(I^*,R^*,\left(\frac{t_{\max}}{\Delta t}-2\right)\Delta t\right)$, and so on. The TER, assuming that a single infectious individual is introduced to the host population at time t_0, is then given by $q_M\left(1,0,t_0\right)$.

We note that, in principle, it would be possible to rearrange system of equations (11) and take the limit $\Delta t \to 0$ to obtain a system of ODEs for $q_M\left(I^*,R^*,t\right)$. However, since we would then be required to discretise time to solve those ODEs numerically, we solve system of equations (11) directly as described above.

2.3.2. Chikungunya transmission model. To compute the TER for the host-vector model, we use a simulation-based approach. Specifically, we repeatedly simulate the analogous stochastic model to system of equations (6), following the simulation procedure described in section 2.1.2. In each simulation, we start with a single infectious host in the population at time t_0. The TER is then given by the proportion of model simulations in which $I_H + R_H$ exceeds or equals M prior to pathogen extinction occurring.

3. Results

3.1. SIR model

To begin comparing the CER and TER, we calculated these quantities for the stochastic SIR model (the analogous stochastic model to system of equations (1)) with a seasonally varying infection rate (equation (2)). We first considered a scenario in which sustained transmission is possible all year round ($R_0(t) > 1$ for all values of t), and set the threshold number of cumulative infections defining a "major outbreak" to be $M = 100$ (corresponding to 10% of the total population size of $N = 1,000$) when calculating the TER. We found that the TER matches the CER closely in that scenario (orange and blue lines in Fig 2A). Not only did we calculate the TER numerically using system of equations (11) (orange line in Fig 2A), but we also calculated the TER using repeated model simulation. To do this, we assumed that there was a single infected individual in the population at the time of pathogen introduction, t_0 (i.e., $S(t_0) = N-1, I(t_0) = 1$ and $R(t_0) = 0$), ran 10,000 simulations of the stochastic SIR

model and then computed the proportion of simulations in which the number of cumulative infections exceeded or equalled $M = 100$ prior to outbreak extinction. We repeated this for a range of values of the time of introduction, t_0 (orange dots in Fig 2A).

While the CER and TER matched closely when transmission was possible all year round (as was the case in previous studies in which the CER was calculated, e.g., [29]), we then went on to consider a second scenario, in which sustained transmission is only possible for some of the year (Fig 2B). In that scenario, outbreaks with at least $M = 100$ cumulative infections were possible for some pathogen introduction times, leading to values of the TER that were greater than and not close to zero (orange line and dots in Fig 2B). However, in the scenario shown in Fig 2B, since pathogen extinction always eventually occurred during time periods in which transmission was not possible, the CER took the value zero at all pathogen introduction times (blue line in Fig 2B).

Although we only considered a single introduced case in Fig 2, we also conducted a supplementary analysis in which we considered multiple pathogen introductions when calculating the TER (S2 Fig).

We then explored the effect of the duration of time in the year for which sustained transmission is impossible ($R_0(t) < 1$) on the mismatch between the CER and TER in more detail. Specifically, we considered different values of β_0 (which represents the mean infection rate across the year) and again calculated the CER and TER (Fig 3).

We found that, if $\beta_0 < \gamma$, then the CER always takes the value zero. However, in those scenarios, but when seasonal transmission is possible, then outbreaks with at least $M = 100$ infections might still occur, leading to substantial differences between the CER and TER (Fig 3A and 3B).
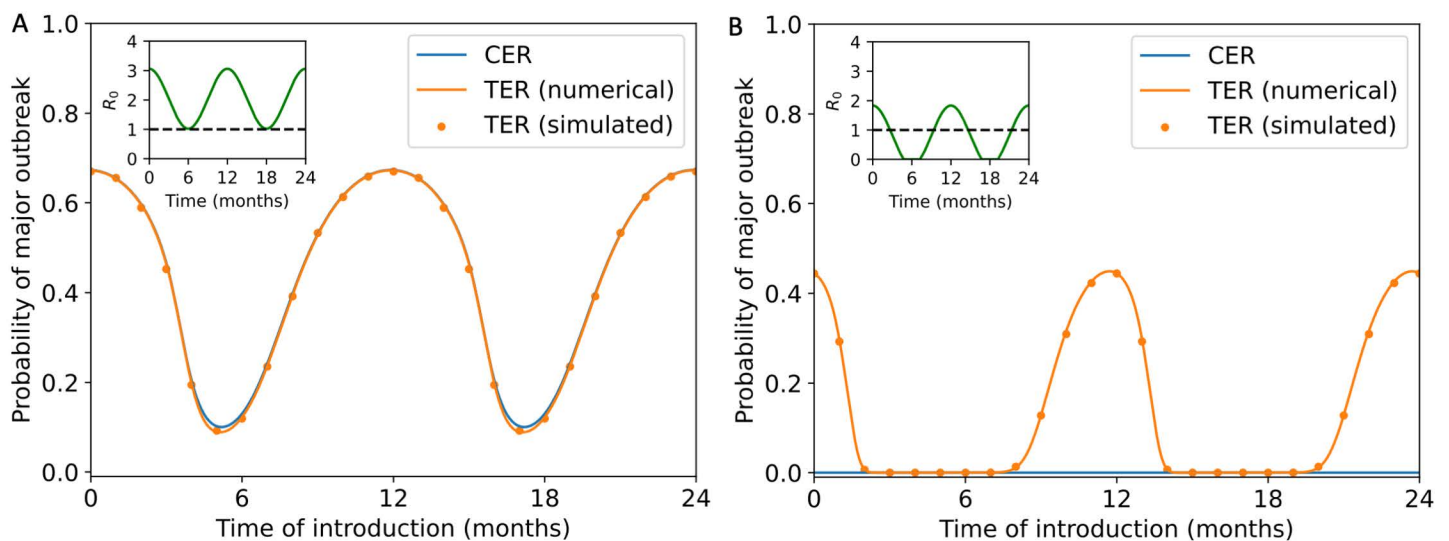

Fig 2. Comparison between calculated values of the CER and TER for the stochastic SIR model with seasonal transmission. A. The CER (obtained using equation (8) – blue line) and the TER (obtained by solving system of equations (11) numerically – orange line – and by running model simulations – orange dots) when sustained transmission is possible throughout the year ($\beta_0 = 10$, $\beta_1 = 5$ and $\gamma = 4.9$ month⁻¹). B. Analogous results to panel A, but in a scenario in which sustained transmission can only occur for some of the year ($\beta_0 = 4$, $\beta_1 = 5$ and $\gamma = 4.9$ month⁻¹). In both panels, a threshold of $M = 100$ was used when computing the TER (analogous results for different values of M are shown in S3 Fig) and the overall population size was assumed to be $N = 1,000$ individuals. When we computed the TER numerically, we used a time step of $\Delta t = 0.00033$ months (i.e., 0.01 days). When we computed the TER using model simulations, we ran 10,000 simulations of the stochastic model (using the simulation approach described in Section 2.1.1) for each time of introduction considered. In both panels, the inset shows $R_0(t) = \beta(t) / \gamma(t)$ as a function of t.

In contrast, if $\beta_0 > \gamma$, then we found that the CER is always strictly positive. However, if there are substantial periods of the year during which sustained transmission cannot occur ($R_0(t) < 1$), then the CER can be vanishingly small. This can include time periods in which the CER is vanishingly small but the TER is substantially greater than zero (Fig 3C and 3D). We also identified some scenarios and time periods in which the CER is substantially greater than zero, yet is still less than the TER (Fig 3C and 3D).

Again, as in Fig 2A, when sustained transmission is possible all year round, or is only impossible for very short periods, then the CER and TER match closely (Fig 3E and 3F).

A similar analysis, but with the extent of seasonality in the infection rate (β_1) varied instead of β_0, is presented in S4 Fig. In that analysis, $\beta_0 > \gamma$, so the CER is always strictly positive (although it is vanishingly small at some times of year in S4D Fig).

Having established that the TER provides a more appropriate characterisation of the risk posed by an invading seasonal pathogen than the CER, we considered the sensitivity of the TER to the precise threshold number of infections, M, chosen (Fig 4). Specifically, we considered both the value of the TER and the duration of the year for which the TER is above a particular value, $z = 0.1$ (in Fig 4, $\beta_0 = 4$). We refer to the latter quantity as the "epidemic risk window". For the transmission parameter values used in Fig 4 ($\beta_1 = 5$, $\gamma = 4.9$ and month^{-1}),

We found that the epidemic risk window differed depending on the value of $M = 200$. For example, if $N = 1{,}000$ was used (corresponding to 20% of the population of $z = 0.1$), then the TER exceeded $M = 400$ for 5.36 months per year, whereas if instead $z = 0.1$ was used (corresponding to 40% of the population), then the TER exceeded for 4.60 months per year. We repeated this analysis for different values of z in S6 Fig. Notably, the start of the epidemic risk window was sensitive to the value of M used, whereas the end of the epidemic risk window was consistent for a range of values of M.

3.2. Chikungunya transmission model

To demonstrate the application of our framework for inferring the risk posed by an invading seasonal pathogen to a real-world case study, we estimated the TER for chikungunya in the town of Feltre, Italy, using daily mean temperature data from 2014 and 2015. The risk that an imported case will initiate a local outbreak varies during the year in that setting due to the seasonal dynamics of the *Ae. albopictus* vector population.

First, we fitted equation (4) to the temperature data from Feltre from 2014 (S1A Fig) and 2015 (S1B Fig). We then used these fitted temperature values to determine the number of adult female vectors per hectare throughout the year, initially by numerically solving system of equations (3) to obtain the number of adult female vectors at the start of each month (blue dots in S1C and S1D Fig) and then by fitting equation (5) to those monthly values (blue lines in S1C and S1D Fig). Finally, we computed the TER in 2014 (Fig 5A) and 2015 (Fig 5B) using model simulations, for a range of different values of the threshold number of cumulative infections defining a major outbreak, $N_V(t)$. In addition to plotting the TER, we computed the CER and found that the CER was either zero (in 2014) or vanishingly small (in 2015) throughout each year due to the extinction of the pathogen during seasons in which environmental conditions are not conducive to transmission. Specifically, outside the summer months, low temperatures drive the vector population size down to a low level, making long-term sustained transmission of chikungunya highly unlikely.

As described in the Methods, in the simulations underlying Fig 5 the temporal dynamics of the adult female vector population (i.e.,) were represented by a skewed, scaled, and shifted
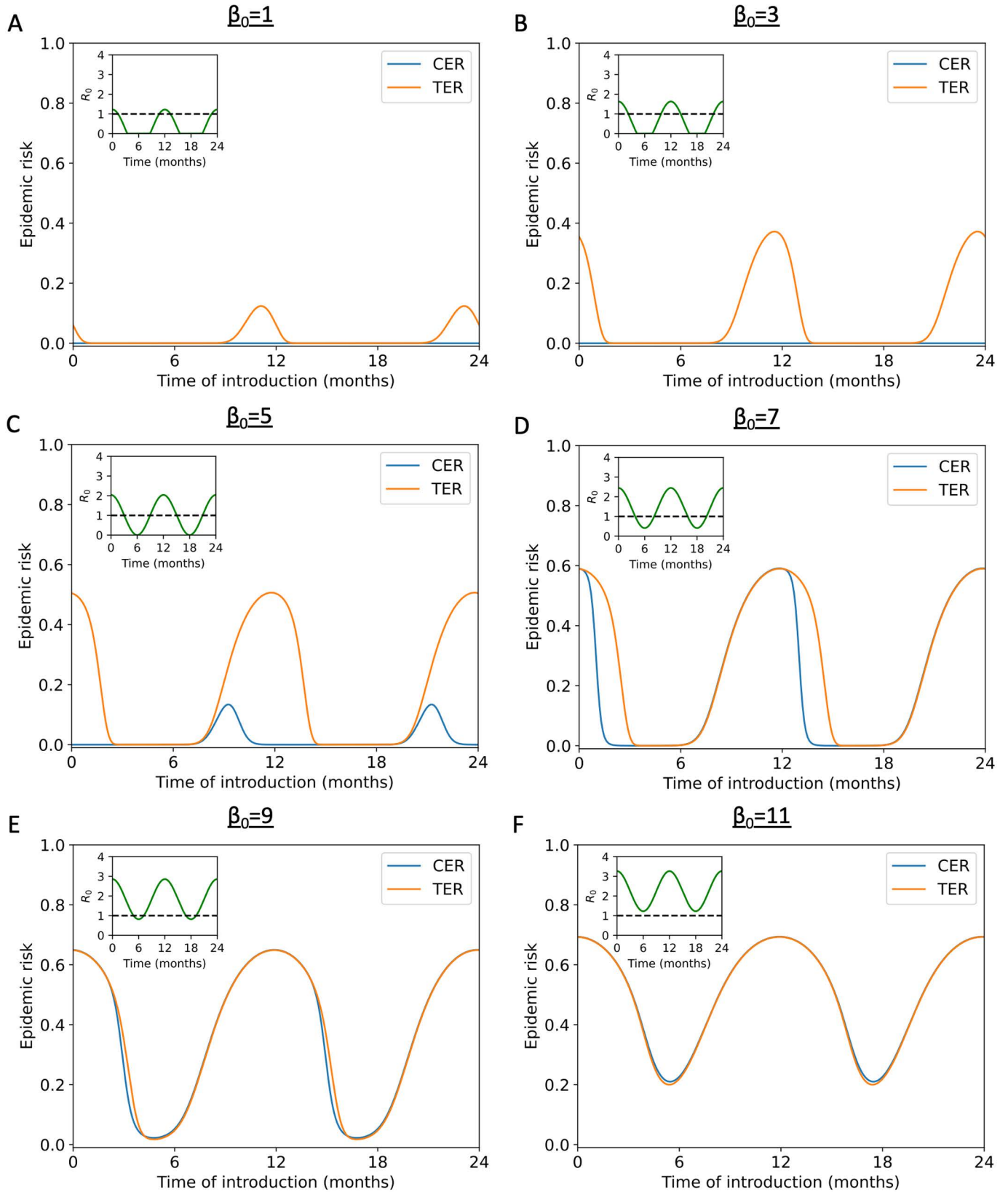
Fig 3. Comparison between calculated values of the CER and TER for the stochastic SIR model with seasonal transmission, for a range of values of β_0. A. The CER (obtained using equation (8) – blue line) and the TER (obtained by solving system of equations (11) numerically – orange line) when sustained transmission

is only possible for a short period of the year ($\beta_0 = 1$, $\beta_1 = 5$ and $\gamma = 4.9$ month^{-1}). B. Analogous results to panel A, but with $\beta_0 = 3$. C. Analogous results to panel A, but with $\beta_0 = 5$. D. Analogous results to panel A, but with $\beta_0 = 7$. E. Analogous results to panel A, but with $\beta_0 = 9$. F. Analogous results to panel A, but with $\beta_0 = 11$. In all panels, a threshold of $M = 100$ and a time step of $\Delta t = 0.00033$ months was used when computing the TER. We confirmed that our results were not sensitive to this choice of Δt by also generating results for $\Delta t = 0.00017$ days; as shown in S5 Fig, our results were unchanged. The overall population size was assumed to be $N = 1,000$ individuals. In all panels, the inset shows $R_0(t) = \beta(t)/\gamma(t)$ as a function of t.
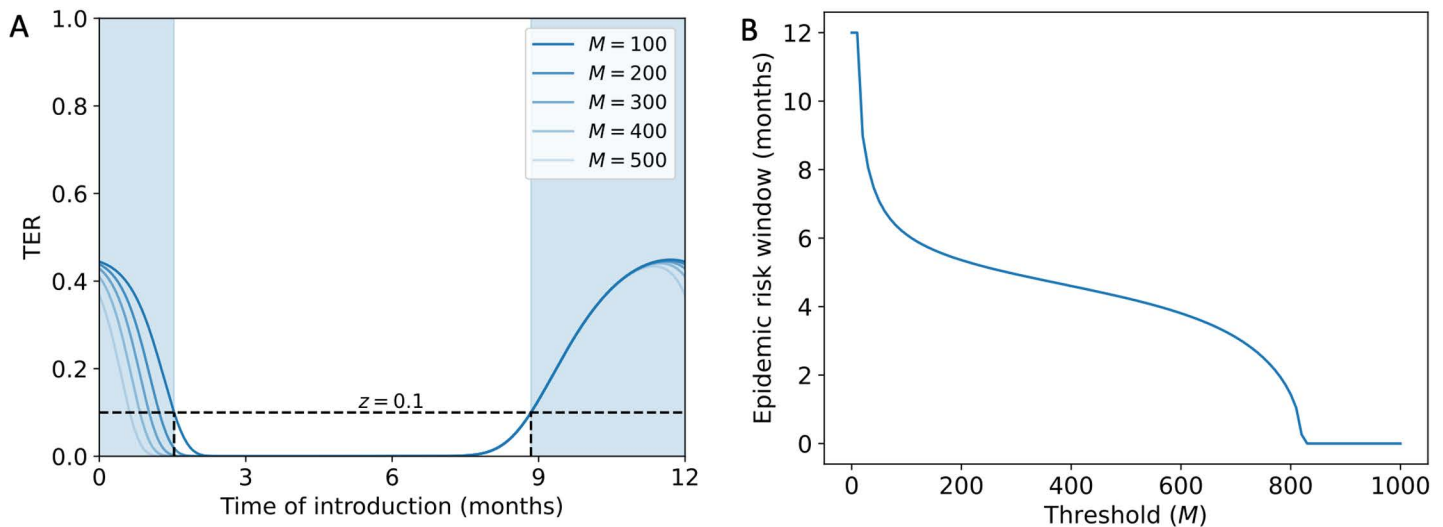
Fig 4. Sensitivity of the TER to the value of *M* chosen for the stochastic SIR model with seasonal transmission. A. The TER (obtained by solving system of equations (11) numerically) for a range of different values of the threshold number of cumulative infections, M. The blue shaded region shows the period of the year for which the TER exceeds $z = 0.1$ for the baseline value of $M = 100$ B. The duration of the year for which the TER exceeds $z = 0.1$ shown as a function of M. In both panels, values of $\beta_0 = 4$, $\beta_1 = 5$ and $\gamma = 4.9$ month^{-1} are used. When we computed the TER numerically, we used a time step of $\Delta t = 0.00033$ months. The overall population size was assumed to be $N = 1,000$ individuals.

Gaussian (equation (5)) that was fitted in each year to the output of the deterministic ecological model (system of equations (3)). To demonstrate the robustness of these results to that approximation, we also calculated the TER using model simulations in which the values of $N_V(t)$ were obtained directly from the numerical solution of the deterministic ecological model; we found that our results were very similar (S7 Fig).

4. Discussion

For many infectious diseases, quantifying the risk that imported cases will initiate a "major outbreak" driven by local transmission is of vital importance for public health policy. This is especially pertinent for seasonal pathogens that are not present at certain times of year, since pathogen reintroduction leading to sustained local transmission is necessary for large numbers of cases to arise. Identification of high-risk locations and time periods allows policymakers to target surveillance and control interventions appropriately.

As described in the Introduction, previous studies have provided methods for calculating the probability of a major outbreak. When transmission parameter values vary temporally, an established method [29,34–41] gives rise to the quantity that we term the CER here. As we have shown, when sustained transmission is possible all year round, the CER provides a useful measure of the risk that an introduced case will initiate local transmission (Figs 2A and 3F). However, when sustained transmission cannot occur for substantial periods of the
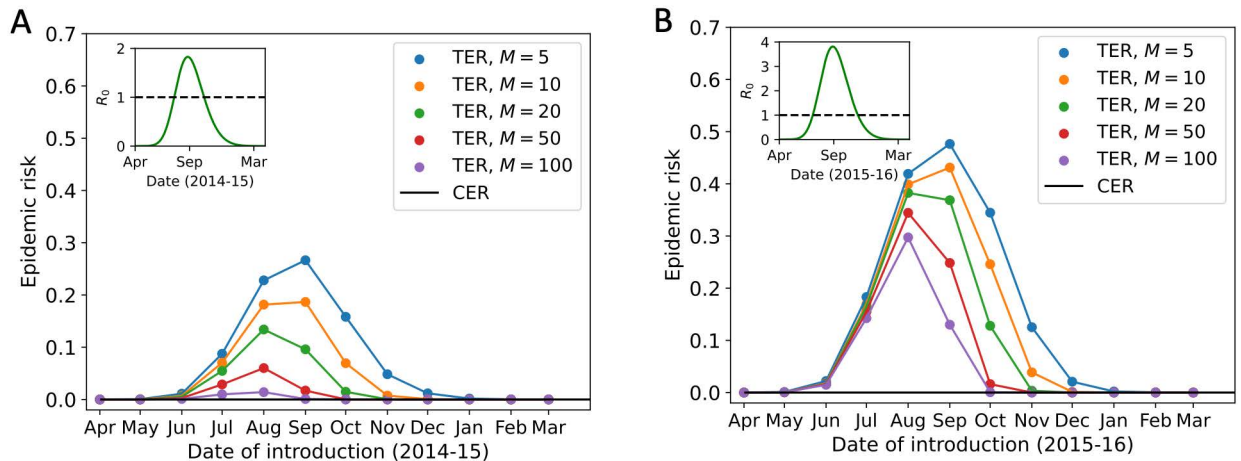
Fig 5. Calculation of the TER for chikungunya in Feltre, northern Italy, in 2014 and 2015. A. The TER for 2014 (and early 2015), shown for a range of values of the threshold number of cumulative infections, M. The CER is also shown (obtained using system of equations (9) – black line). B. Analogous to panel A, but for 2015 (and early 2016). In both panels, to compute the CER we ran 10,000 simulations of the stochastic model (using the simulation approach described in Section 2.1.2) for each date of introduction considered. The host population size was assumed to be $N = 5,000$ individuals (based on the population density in Feltre [44], this corresponds to an area of 80 Ha; the numbers of adult female vectors were also scaled up from their per Ha values shown in S1C and S1D Fig). In both panels, the inset shows $R_0(t)$ as a function of t (equation (7)).

https://doi.org/10.1371/journal.pcbi.1012364.g005

year (e.g., over winter, as is the case for vector-borne pathogens in temperate climates such as southern Europe), then the CER can underestimate the true risk of a substantial outbreak occurring, including scenarios and time periods in which outbreaks with large numbers of cases can begin yet the CER takes the value zero (Figs 2B, 3A and 3B) or is vanishingly small (Fig 3C and 3D). For this reason, we have proposed a different quantity (the TER) that can be calculated to assess the probability of a major outbreak. Specifically, the TER represents the probability that introduced cases initiate an outbreak with at least R_0 infections prior to outbreak extinction.

The risk of an outbreak occurring in which a threshold number of cumulative cases is exceeded has been considered in some previous studies. For example, for models in which transmission parameter values do not vary temporally, Thompson *et al.* [30] showed that the TER tends to match classic estimates for the probability of a major outbreak for a range of values of M, at least when is sufficiently larger than one. Robert *et al.* [51] considered transmission of dengue in Miami and computed the TER (there termed the "probability of autochthonous transmission") via repeated simulation of a stochastic model, including considering the risk of outbreaks of different sizes. However, the key extension of the current study is to compare calculations of the TER against calculations of the CER for seasonal pathogens, highlighting that the TER provides a more practically useful quantification of the risk posed by seasonal pathogens.

We found that the precise value of M chosen affects the calculated value of the TER and the inferred duration of the year for which the outbreak risk is heightened (Fig 4). This in fact motivates the use of the TER as a practical epidemic risk metric to guide decision making, since it would be possible for policy advisors to choose the value of M that is most appropriate for the context under consideration. For example, for a pathogen such as dengue virus in Italy, even relatively small outbreaks would be considered substantial. Since 2010, the majority of dengue outbreaks in mainland Europe have consisted of fewer than 40 cases [52]. Therefore,

even outbreaks of size 10–20 might be considered large in that setting, suggesting that a value of M of that size might be appropriate. By choosing a value of M that is suitable for a specific pathogen and location, the epidemic risk window can be calculated (as in Fig 4) and used to inform the timing of interventions. Consequently, if mathematical modellers undertake calculation of the TER, then we contend that this should be done for any specific outbreak in consultation with policy specialists, to ensure that an appropriate value of M is used. Alternatively, the TER could be computed for a range of values of M, so that estimates of the risk of outbreaks of a range of different sizes are obtained.

As we showed by applying our approach to the case study of chikungunya in northern Italy (Fig 5), the methodology presented here is particularly relevant in the context of vector-borne diseases in locations that experience seasonal outbreaks. Going forwards, the risk of vector-borne disease outbreaks is expected to increase in some locations due to climate change [53–55]. Calculation of the TER across a range of places and at different times of year can provide insights into changes in the spatio-temporal risk of outbreaks and support the adoption of preventive measures [44]. In addition to demonstrating that the CER does not provide an appropriate assessment of the risk of seasonal outbreaks in some real-world scenarios, two features are particularly noticeable from our TER calculations in Fig 5. First, relatively small differences in temperature between years (S1A and S1B Fig) can drive more substantial differences in the vector population size (S1C and S1D Fig), and therefore in the risk posed by outbreaks. Second, the choice of value of M affects the time of pathogen introduction at which the TER is maximised. Specifically, larger values of M require longer outbreaks for the threshold number of cumulative infections to be exceeded. As a result, larger values of M tend to lead to earlier peak values of the TER, in order for there to be sufficient time left in the transmission season for such large outbreaks to occur. We note that, early in the transmission season, the TER can be consistent across a range of values of M (Fig 5B). This is because, once a small threshold number of cumulative cases is exceeded, a large outbreak may be guaranteed. On the other hand, near the end of the season, the TER varies more substantially with $z = 0.1$. This is because, even if a smaller threshold number of cumulative infections is exceeded, a larger threshold may not go on to be exceeded because sustained transmission will soon become impossible.

When considering the host-vector model of chikungunya virus transmission, we chose to use a simulation-based approach for computing the TER as opposed to the numerical approach that we used in the case of the SIR model. We did this to demonstrate the extensibility of our framework to epidemiological models with any level of complexity (although we note that, for very complex stochastic epidemiological models with large numbers of events, a limitation of our approach is that repeated model simulation could require substantial computational resource). Future applications of the TER could consider more detailed host-vector models. For example, parameters such as the extrinsic incubation period could be assumed to vary with temperature [56,57]. Alternatively, the utility of the TER in entirely different scenarios could be analysed, for example by considering seasonal respiratory outbreak pathogens. The dynamics of directly transmitted childhood infections, such as the varicella-zoster virus (the causative agent of chickenpox), are affected by school terms [58], and the TER might be a useful metric for quantifying the risk of "within-term" outbreaks of different sizes. Additionally, the TER might sometimes be a useful metric even if seasonal dynamics are not considered. For example, the high case fatality rate observed during past Ebola virus disease outbreaks means that even outbreaks with relatively small numbers of cases might be classified as "major", motivating the use of the TER with a relatively small value of $M = 100$. Finally, we note that a benefit of using the TER to quantify outbreak risks is that it is possible to account for temporal changes in the offspring distribution due to factors such as local depletion of susceptible individuals. In fact,

any complexity in real-world systems can be built into simulation-based calculation of the TER by simply including the relevant features in the simulation model; considering such extensions, including ensuring that temporal changes in offspring distributions are reflected accurately in epidemiological models, is a key target for future research.

In summary, we have developed a novel framework for seasonal pathogens that can be used to compute the probability that an initial infected case (or cases) initiates a "major outbreak". Rather than basing our approach on the mathematical theory of branching processes, which can lead to unrealistic assessments of seasonal outbreak risks, we calculate the TER (i.e., the probability that the number of cumulative infections will exceed a pre-specified threshold value). For simple stochastic epidemic models that account for seasonality, the TER can be calculated numerically. For more complex models, the TER can be estimated using model simulations, enabling it to be determined for any epidemiological system for which repeated model simulation is possible. Going forwards, we hope that our flexible approach will be used by epidemiological modellers to obtain policy-relevant outbreak risk assessments for a range of pathogens.

Supporting information

S1 Text. Supplementary text for *Quantifying infectious disease epidemic risks: A practical approach for seasonal pathogens.*
(DOCX)

S1 Fig. Temperature and vector density in Feltre, Northern Italy, in 2014 and 2015. A. Daily mean temperature in Feltre in 2014 as sourced from MODIS satellite Land Surface Temperature measurements (blue line) and smoothed temperature values obtained by fitting equation [(4)](#) in the main text to those data (orange line). B. Analogous to panel A, but using temperature data from 2015. C. Monthly number of adult female vectors per hectare in 2014 (and early 2015) obtained by solving system of equations [(3)](#) in the main text numerically based on the fitted temperature values in panel A (blue dots), and inferred number of adult female vectors per hectare obtained by fitting equation [(5)](#) in the main text to the monthly values (blue line). The ecological model is initialised at the beginning of April 2014. The fitted values shown from January to March 2014 reflect the fit from early 2015 (assuming annual periodicity). D. Analogous to panel C, but for 2015 (and early 2016), based on the fitted temperature values in panel B.
(PDF)

S2 Fig. Dependence of the TER on the initial number of infected individuals, for the stochastic SIR model with seasonal transmission. A. The TER for different initial numbers of infectious individuals (obtained by solving system of equations [(11)](#) in the main text numerically). B. The duration of the year for which the TER exceeds $\Delta t = 0.00033$, for different initial numbers of infectious individuals. In both panels, a threshold of $N = 1{,}000$ cumulative infections and a time step of $\beta_0 = 4$ months was used when computing the TER. The overall population size was assumed to be $\beta_1 = 5$ individuals. Parameter values used: $\gamma = 4.9$, and $\beta_1 = 5$ month^{-1}.
(PDF)

S3 Fig. Dependence of the TER on the value of *M* used, for the stochastic SIR model with seasonal transmission. A. The TER (obtained by solving system of equations [(11)](#) numerically) when sustained transmission is possible throughout the year ($\gamma = 4.9$, and $\beta_0 = 4$ month^{-1}), for different values of $\beta_1 = 5$ (100, 200, 300, 400 and 500). For $\gamma = 4.9$, the TER as approximated using model simulations is also plotted (blue dots). B. Analogous results to

panel A, but in a scenario in which sustained transmission can only occur for some of the year ($N = 1,000$, $\Delta t = 0.00033$ and $10,000$ month^{-1}). In both panels, the overall population size was assumed to be β_1 individuals. When we computed the TER numerically, we used the time step $\beta_0 = 10$ months. When we approximated the TER using model simulations, $\beta_1 = 0$ simulations were run for each time of introduction considered.
(PDF)

S4 Fig. Comparison between calculated values of the CER and TER for the stochastic SIR model with seasonal transmission, for a range of values of $\gamma = 4.9$. A. The CER (obtained using equation (8) in the main text; blue line) and the TER (obtained by solving system of equations (11) in the main text numerically; orange line) when $\beta_1 = 3$, $\beta_1 = 6$ and $\beta_1 = 9$ month^{-1}. B. Analogous results to panel A, but with $M = 100$. C. Analogous results to panel A, but with $\Delta t = 0.00033$. D. Analogous results to panel A, but with $N = 1,000$. In all panels, a threshold of $R_0(t) = \beta(t) / \gamma(t)$ and a time step of $R_0(t) = \beta(t) / \gamma(t)$ months was used when computing the TER. The overall population size was assumed to be individuals. Insets show $\beta_0 = 1$ as a function of $\beta_1 = 5$.
(PDF)

S5 Fig. Comparison between numerically computed values of the TER for two different values of the time step, $\gamma = 4.9$, for the stochastic SIR model with seasonal transmission. A. The TER (obtained by solving system of equations (11) from the main text numerically) when sustained transmission is only possible for a short period of the year ($\Delta t = 0.00033$, $\Delta t = 0.00017$ and $\beta_0 = 3$ month^{-1}). Results are shown for both the time step used in the main text ($\beta_0 = 5$ months; blue line) and for a shorter time step ($\beta_0 = 7$ months; black dotted line). B. Analogous results to panel A, but with $\beta_0 = 9$. C. Analogous results to panel A, but with $\beta_0 = 11$. D. Analogous results to panel A, but with $M = 100$. E. Analogous results to panel A, but with $N = 1,000$. F. Analogous results to panel A, but with $R_0(t) = \beta(t) / \gamma(t)$. In all panels, a threshold of $R_0(t) = \beta(t) / \gamma(t)$ cumulative infections was used when computing the TER and the overall population size was assumed to be individuals. Insets show as a function of .
(PDF)

S6 Fig. Duration of the year for which the TER exceeds z in the stochastic SIR model with seasonal transmission, for a range of values of M and z $M = 100$. A. The TER (obtained by solving system of equations (11) in the main text numerically) for a range of different values of the threshold number of infections, $z = 0.4$. The blue shaded region shows the period of the year for which the TER exceeds $z = 0.4$ when ,. B. The duration of the year for which the TER exceeds , shown as a function of M. C. Heatmap indicating the duration of the year for which the TER exceeds , shown for a range of values of $\beta_1 = 5$ and $\gamma = 4.9$. In all panels, values of $\Delta t = 0.00033$, $N = 1,000$ and $N = 1,000$ month^{-1} are used. A time step of months was used when computing the TER. The overall population size was assumed to be $N = 5,000$ individuals.
(PDF)

S7 Fig. Calculation of the TER for. chikungunya in Feltre, Northern Italy, in 2014 and 2015, with and without the approximation in equation (5) of the main text. A. The TER for 2014, shown for a range of values of the threshold number of cumulative infections, $N = 5,000$. The TER computed using the approximation in equation (5) of the main text (as in Fig 5 of the main text; dashed lines) is compared to the TER computed using values of obtained directly from the numerical solution of the deterministic ecological model (system

of equations (3) in the main text; solid lines). B. Analogous to panel A, but for 2015. In both panels, we ran 10,000 simulations of the stochastic model (using the simulation approach described in Section 2.1.2 of the main text) for each date of introduction considered. The host population size was assumed to be individuals (based on the population density in Feltre, this corresponds to an area of 80 Ha, and the numbers of adult female vectors (shown in S1C and S1D Fig) were scaled up from their per Ha values accordingly).
(PDF)

Acknowledgments

Author contributions

Conceptualization: Alexander R. Kaye, Robin N. Thompson.

Formal analysis: Alexander R. Kaye.

Investigation: Alexander R. Kaye.

Methodology: Alexander R. Kaye, Giorgio Guzzetta, Robin N. Thompson.

Project administration: Robin N. Thompson.

Software: Alexander R. Kaye.

Supervision: Michael J. Tildesley, Robin N. Thompson.

Validation: Alexander R. Kaye.

Writing – original draft: Alexander R. Kaye, Robin N. Thompson.

Writing – review & editing: Alexander R. Kaye, Giorgio Guzzetta, Michael J. Tildesley, Robin N. Thompson.

References

1. Smith KF, Goldberg M, Rosenthal S, Carlson L, Chen J, Chen C, et al. Global rise in human infectious disease outbreaks. J R Soc Interface. 2014;11(101):20140950. https://doi.org/1098/rsif.2014.0950 PMID: 25401184

2. Bloom DE, Cadarette D. Infectious disease threats in the twenty-first century: strengthening the global response. Front Immunol. 2019;10:549. https://doi.org/3389/fimmu.2019.00549 PMID: 30984169

3. Tatem AJ, Rogers DJ, Hay SI. Global transport networks and infectious disease spread. Adv Parasitol. 2006;62:293–343. https://doi.org/1016/S0065-308X(05)62009-X PMID: 16647974

4. Baker RE, Mahmud AS, Miller IF, Rajeev M, Rasambainarivo F, Rice BL, et al. Infectious disease in an era of global change. Nat Rev Microbiol. 2022;20(4):193–205. https://doi.org/1038/s41579-021-00639-z PMID: 34646006

5. Massad E, Amaku M, Coutinho FAB, Struchiner CJ, Burattini MN, Khan K, et al. Estimating the probability of dengue virus introduction and secondary autochthonous cases in Europe. Sci Rep. 2018;8(1):4629. https://doi.org/1038/s41598-018-22590-5 PMID: 29545610

6. Guzzetta G, Vairo F, Mammone A, Lanini S, Poletti P, Manica M, et al. Spatial modes for transmission of chikungunya virus during a large chikungunya outbreak in Italy: a modeling analysis. BMC Med. 2020;18(1):226. https://doi.org/1186/s12916-020-01674-y PMID: 32762750

7. Hotez PJ. Southern Europe's coming plagues: vector-borne neglected tropical diseases. PLoS Negl-Trop Dis. 2016;10(6):e0004243. https://doi.org/1371/journal.pntd.0004243

8. Guzzetta G, Montarsi F, Baldacchino FA, Metz M, Capelli G, Rizzoli A, et al. Potential risk of dengue and chikungunya outbreaks in Northern Italy based on a population model of *Aedes albopictus* (Diptera: Culicidae). PLoS NeglTrop Dis. 2016;10(6):e0004762. https://doi.org/1371/journal.pntd.0004762 PMID: 27304211

9. Alto BW, Juliano SA. Precipitation and temperature effects on populations of *Aedes albopictus* (Diptera: Culicidae): implications for range expansion. J Med Entomol. 2001;38(5):646–56. https://doi.org/1603/0022-2585-38.5.646 PMID: 11580037

10. Juliano SA, O'Meara GF, Morrill JR, Cutwa MM. Desiccation and thermal tolerance of eggs and the coexistence of competing mosquitoes. Oecologia. 2002;130(3):458–69. https://doi.org/1007/s004420100811 PMID: 20871747

11. Yang HM, Macoris MLG, Galvani KC, Andrighetti MTM, Wanderley DMV. Assessing the effects of temperature on the population of *Aedes aegypti*, the vector of dengue. Epidemiol Infect. 2009;137(8):1188–202. https://doi.org/1017/S0950268809002040 PMID: 19192322

12. Kraemer MUG, Reiner RC, Brady OJ, Messina JP, Gilbert M, Pigott DM, et al. Past and future spread of the arbovirus vectors *Aedes aegypti* and *Aedes albopictus*. Nat Microbiol. 2019;4(5):854–63. https://doi.org/1038/s41564-019-0376-y PMID: 30833735

13. Antia R, Regoes RR, Koella JC, Bergstrom CT. The role of evolution in the emergence of infectious diseases. Nature. 2003;426(6967):658–61. https://doi.org/1038/nature02104 PMID: 14668863

14. Meehan MT, Cope RC, McBryde ES. On the probability of strain invasion in endemic settings: accounting for individual heterogeneity and control in multi-strain dynamics. J Theor Biol. 2020;487:110109. https://doi.org/1016/j.jtbi.2019.110109 PMID: 31816294

15. Hartfield M, Alizon S. Epidemiological feedbacks affect evolutionary emergence of pathogens. Am Nat. 2014;183(4): E105–17. https://doi.org/1086/674795 PMID: 24642501

16. Yates A, Antia R, Regoes RR. How do pathogen evolution and host heterogeneity interact in disease emergence? Proc Biol Sci. 2006;273(1605):3075–83. https://doi.org/1098/rspb.2006.3681 PMID: 17015347

17. Lloyd-Smith JO, Schreiber SJ, Kopp PE, Getz WM. Superspreading and the effect of individual variation on disease emergence. Nature. 2005;438(7066):355–9. https://doi.org/1038/nature04153 PMID: 16292310

18. Lovell-Read FA, Funk S, Obolski U, Donnelly CA, Thompson RN. Interventions targeting non-symptomatic cases can be important to prevent local outbreaks: SARS-CoV-2 as a case study. J R Soc Interface. 2021;18(178): 20201014. https://doi.org/1098/rsif.2020.1014 PMID: 34006127

19. Lahodny GE Jr, Gautam R, Ivanek R. Estimating the probability of an extinction or major outbreak for an environmentally transmitted infectious disease. J Biol Dyn. 2015;9(Suppl 1):128–55. https://doi.org/1080/17513758.2014.954763 PMID: 25198247

20. Sachak-Patwa R, Byrne HM, Dyson L, Thompson RN. The risk of SARS-CoV-2 outbreaks in low prevalence settings following the removal of travel restrictions. Commun Med. 2021;1:39. https://doi.org/1038/s43856-021-00038-8 PMID: 35602220

21. Thompson RN, Lovell-Read FA, Obolski U. Novel coronavirus outbreak in Wuhan, China, 2020: intense surveillance is vital for preventing sustained transmission in new locations. J Clin Med. 2020;9(5):1297. https://doi.org/3390/jcm9051297 PMID: 32369975

22. Lahodny GE Jr, Allen LJS. Probability of a disease outbreak in stochastic multipatch epidemic models. Bull Math Biol. 2013;75(7):1157–80. https://doi.org/1007/s11538-013-9848-z PMID: 23666483

23. Leventhal GE, Hill AL, Nowak MA, Bonhoeffer S. Evolution and emergence of infectious diseases in theoretical and real-world networks. Nat Commun. 2015;6: 6101. https://doi.org/1038/ncomms7101 PMID: 25592476

24. Anderson D, Watson R. On the spread of a disease with gamma distributed latent and infectious periods. Biometrika. 1980;67(1):191. https://doi.org/2307/2335333

25. Lovell-Read FA, Shen S, Thompson RN. Estimating local outbreak risks and the effects of non-pharmaceutical interventions in age-structured populations: SARS-CoV-2 as a case study. J Theor Biol. 2022;535: 110983. https://doi.org/1016/j.jtbi.2021.110983 PMID: 34915042

26. Nishiura H, Cook AR, Cowling BJ. Assortativity and the probability of epidemic extinction: a case study of pandemic influenza a (H1N1-2009). Interdiscip Perspect Infect Dis. 2011;2011:194507. https://doi.org/1155/2011/194507 PMID: 21234337

27. Mugabi F, Duffy KJ, Mugisha JYT, Collins OC. Determining the effects of wind-aided midge movement on the outbreak and coexistence of multiple bluetongue virus serotypes in patchy environments. Math Biosci. 2021;342: 108718. https://doi.org/1016/j.mbs.2021.108718 PMID: 34666068

28. Lloyd AL, Zhang J, Root AM. Stochasticity and heterogeneity in host-vector models. J R Soc Interface. 2007;4(16):851–63. https://doi.org/1098/rsif.2007.1064 PMID: 17580290

29. Kaye AR, Hart WS, Bromiley J, Iwami S, Thompson RN. A direct comparison of methods for assessing the threat from emerging infectious diseases in seasonally varying environments. J Theor Biol. 2022;548:111195. https://doi.org/1016/j.jtbi.2022.111195 PMID: 35716723

30. Thompson RN, Gilligan CA, Cunniffe NJ. Will an outbreak exceed available resources for control? Estimating the risk from invading pathogens using practical definitions of a severe epidemic: will an outbreak exceed available resources for control? Estimating the risk from invading pathogens using practical definitions of a severe epidemic. J R Soc Interface. 2020;17(172):20200690. https://doi.org/1098/rsif.2020.0690 PMID: 33171074

31. Althaus CL, Low N, Musa EO, Shuaib F, Gsteiger S. Ebola virus disease outbreak in Nigeria: transmission dynamics and rapid control. Epidemics. 2015;11:80–4. https://doi.org/1016/j.epidem.2015.03.001 PMID: 25979285

32. Hellewell J, Abbott S, Gimma A, Bosse NI, Jarvis CI, Russell TW, et al; Centre for the Mathematical Modelling of Infectious Diseases COVID-19 Working Group. Feasibility of controlling COVID-19 outbreaks by isolation of cases and contacts. Lancet Glob Health. 2020;8(4):e488–96. https://doi.org/1016/S2214-109X(20)30074-7 PMID: 32119825

33. Thompson RN, Thompson MJ, Hurrell JW, Sun L, Obolski U. Assessing the threat of major outbreaks of vector-borne diseases under a changing climate. Astrophysics and Space Science Proceedings. Springer Science and Business Media B.V.; 2020. pp. 25–35. https://doi.org/1007/978-3-030-55336-4_5

34. Kendall DG. On the generalized "birth-and-death" process. Ann Math Stat. 1948;19:1–15. https://doi.org/1214/aoms/1177730285

35. Nipa KF, Allen LJS. Disease emergence in multi-patch stochastic epidemic models with demographic and seasonal variability. Bull Math Biol. 2020;82(12):152. https://doi.org/1007/s11538-020-00831-x PMID: 33231753

36. Ball F. The threshold behaviour of epidemic models. J Appl Probab. 1983;20(02):227–41. https://doi.org/1017/s0021900200023391

37. Bacaër N, Ait Dads EH. On the probability of extinction in a periodic environment. J Math Biol. 2014;68(3):533–48. https://doi.org/1007/s00285-012-0623-9 PMID: 23143337

38. Bacaër N, Ed-Darraz A. On linear birth-and-death processes in a random environment. J Math Biol. 2014;69(1):73–90. https://doi.org/1007/s00285-013-0696-0 PMID: 23728211

39. Bacaër N. Deux modèles de population dans un environnement périodique lent ou rapide. J Math Biol. 2020;80(4):1021–37. https://doi.org/1007/s00285-019-01447-z

40. Carmona P, Gandon S. Winter is coming: pathogen emergence in seasonal environments. PLoS Comput Biol. 2020;16(7):e1007954. https://doi.org/1371/journal.pcbi.1007954 PMID: 32628658

41. Bacaër N, Lobry C, Sari T. Sur la probabilité d'extinction d'une population dans un environnement périodique lent. ARIMA J. 2020;32:81–95.

42. Wang X, Saad-Roy CM, van den Driessche P. Stochastic model of Bovine Babesiosis with juvenile and adult cattle. Bull Math Biol. 2020;82: https://doi.org/1007/s11538-020-00734-x

43. Thompson RN, Jalava K, Obolski U. Sustained transmission of Ebola in new locations: more likely than previously thought. Lancet Infect Dis. 2019;19(10):1058–9. https://doi.org/1016/S1473-3099(19)30483-9 PMID: 31559960

44. Guzzetta G, Trentini F, Poletti P, Baldacchino FA, Montarsi F, Capelli G, et al. Effectiveness and economic assessment of routine larviciding for prevention of chikungunya and dengue in temperate urban settings in Europe. PLoS NeglTrop Dis. 2017;11(9):e0005918. https://doi.org/1371/journal.pntd.0005918 PMID: 28892499

45. Norris JR. Markov Chains. Cambridge University Press; 1997. https://doi.org/1017/CBO9780511810633

46. Garrido M, Veiga J, Garrigós M, Morales-Yuste M, Recuero-Gil J, Martínez-de la Puente J. *Aedes albopictus* in a recently invaded area in Spain: effects of trap type, locality, and season on mosquito captures. Sci Rep. 2024;14(1): https://doi.org/1038/s41598-024-52040-4

47. Gillespie DT. Exact stochastic simulation of coupled chemical reactions. J Phys Chem. 1977; https://doi.org/1021/j100540a008

48. Thanh VH, Priami C. Simulation of biochemical reactions with time-dependent rates by the rejection-based algorithm. J Chem Phys. 2015;143(5):054104. https://doi.org/1063/1.4927916 PMID: 26254639

49. Mastin AJ, Gottwald TR, van den Bosch F, Cunniffe NJ, Parnell S. Optimising risk-based surveillance for early detection of invasive plant pathogens. PLoS Biol. 2020;18(10):e3000863. https://doi.org/1371/journal.pbio.3000863 PMID: 33044954

50. Driscoll TA, Hale N. Chebfun Guide. Oxford: Pafnuty Publications; 2014.

51. Robert MA, Christofferson RC, Silva NJB, Vasquez C, Mores CN, Wearing HJ. Modeling mosquito-borne disease spread in U.S. urbanized areas: the case of dengue in Miami. PLoS One. 2016;11(8):e0161365. https://doi.org/1371/journal.pone.0161365 PMID: 27532496

52. European Centre for Disease Prevention and Control. Local transmission of dengue virus in mainland EU/EEA, 2010-present; 2024. Available from: https://www.ecdc.europa.eu/en/all-topics-z/dengue/surveillance-and-disease-data/autochthonous-transmission-dengue-virus-eueea

53. Ryan SJ, Carlson CJ, Mordecai EA, Johnson LR. Global expansion and redistribution of *Aedes*-borne virus transmission risk with climate change. PLoS NeglTrop Dis. 2018;13(3):e0007213. https://doi.org/1371/journal.pntd.0007213

54. Fischer D, Thomas SM, Niemitz F, Reineking B, Beierkuhnlein C. Projection of climatic suitability for *Aedes albopictus* Skuse (Culicidae) in Europe under climate change conditions. Glob Planet Change. 2011;78(1-2):54–64. https://doi.org/1016/j.gloplacha.2011.05.008

55. Kaye AR, Obolski U, Sun L, Hart WS, Hurrell JW, Tildesley MJ, et al. The impact of natural climate variability on the global distribution of *Aedes aegypti*: a mathematical modelling study. Lancet Planet Health. 2024;8(12):e1079–87. https://doi.org/1016/S2542-5196(24)00238-9 PMID: 39674197

56. Liu Z, Zhang Q, Li L, He J, Guo J, Wang Z, et al. The effect of temperature on dengue virus transmission by *Aedes* mosquitoes. Front Cell Infect Microbiol. 2023;13: https://doi.org/3389/fcimb.2023.1320461

57. Delrieu M, Martinet J-P, O'Connor O, Viennet E, Menkes C, Buret-Sarramegna V, et al. Temperature and transmission of chikungunya, dengue, and Zika viruses: a systematic review of experimental studies on *Aedes aegypti* and *Aedes albopictus*. Curr Res Parasitol Vector-Borne Diseas. 2023;4:100139. https://doi.org/1016/j.crpvbd.2023.100139 PMID: 37719233

58. Jackson C, Mangtani P, Fine P, Vynnycky E. The effects of school holidays on transmission of varicella zoster virus, England and Wales, 1967–2008. PLoS One. 2014;9(6):e99762. https://doi.org/1371/journal.pone.0099762 PMID: 24932994